Chapter 3

Evolution of weak discontinuity waves in non-ideal interstellar environments *

3.1 Introduction

A systematic method is used to study the problem of propagation of planar, cylindrically symmetric and spherically symmetric shock waves of the one-dimensional motion of an inviscid, self-gravitating, non-ideal interstellar gas cloud. Most of the physical phenomena occurring in compressible fluids are non-linear which may be modelled mathematically in the form of non-linear partial differential equations (PDEs). Such PDEs contribute to many problems of supersonic flows, plasma flows,

* "The contents of this chapter have been published in ***Zeitschrift für Naturforschung A (De Gruyter), 2022.***"

interstellar flows, aerospace science, space research, astrophysics and many more. Laws of mechanics and thermodynamics forms the theoretical basis of gas dynamics. Shock wave arise due to sudden changes in the flow variables. It's study has great significance in innumerable fields and in recent years, its practical importance has risen due to its specific applications in astrometry, uranology, nuclear physics, geology, seismology, and their applications to the satellite's motion. Due to energetic events like the collision of clouds, stellar winds, powerful and luminous stellar explosion, supernova blast, rapid crashes between interstellar gas clusters, remarkably high rate of star formation, etc., the shock waves become usual in the interstellar medium. The authors (Courant and Friedrichs [3],Lax [98], Chen and Gurtin [99], Pandey [100], Shyam et al. [101], Shah et al.[102],Chaturvedi et al. [103], Modelevsky nad Sari [104]) have used several analytical apporaches to study the phenomena of shock formation, diverging and converging shock waves, growth and deteriorating behavior of shocks and propagation of shock wave in several regime. Nath and Singh [105] studied the evolution of cylindrical shocks with isothermal flow condition using power series method. Maslov and Tsupin [106] proposed a new method to depict the geometry of movement of shocks in an isentropic gas using the universal method of difference schemes. Higashino [107] studied non-uniform propagation of blast wave and shock tube problem using Hartree's method in dusty gas cloud. Nath [108] investigated explosion problems for cylindrical and spherical symmetry cases. Singh and Arora [109] have studied one-dimensional shocks, with the help of infinite hierarchy of the transport equation and truncation approximation method in the presence of radiating gas. The kinametics of cylindrical shocks in rotationally axisymmetric non-ideal gas was studied by Nath et al. [110]. In order to examine the evolution of shocks, Singh and Arora [111] used the power series method and discussed the impact of shock Cowling number and non-ideal parameter on flow variables. Various studies on other facts about shocks are done by many authors in the literature (see Refs. Singh et al.[112], Srivastava et al. ([113] ,[97]), Gupta et al. [96]).

A commonly occurring situation for the problems related to shocks is lower temperatures and high pressures, where ideal gas assumptions are no longer valid. Then the model of non-ideal gas is the prevailing substitute model for it. Robert and Wu [114] and Wu and Robert [115] adopted the van der Waals model and discussed the theory of shock waves of sonoluminescence. Gupta et al. [116] investigated one-dimensional unsteady cylindrical shocks in non-ideal gas with isothermal flow. Sahu [117] considered gravity field, variable magnetic field, radiation flux, thermal conduction for self-similar solution originated through travelling piston in non-ideal gas filled with dust. Nath [118] proposed evolution of shocks of micro-size dust particles with monochromatic radiation. The authors in Arora and Siddiqui [119] have derived the transport equation to discuss the evolutionary behavior of planar, cylindrical, and spherical weak shocks in the non-ideal medium. Arora et al. [120] have worked on the collapse of imploding cylindrically and spherically symmetric shocks to obtain solutions of shock waves of strong strength in non-ideal gas. Related articles for the study of shock wave solutions in non-ideal gasdynamics can be seen in Pandey and Sharma [121], Singh et al. [81], Bira et al. [122], Nath and Vishwakarma [123]. Various phenomena in space research and astronomical physics, including the gravitational collapse in the interstellar medium, are significant due to the description of star-forming regions. Hence, study of collapse of a self-gravitating interstellar gas cloud in the spiral arms of the Galaxy has shifted the attention of astrophysicists as they had an interest in patterns of stellar systems, stars, and supernova explosions. The study of interstellar gas dynamics is important for understanding the energy budget, structure, and evolution of the interstellar medium. Interstellar medium is intermittently disturbed by violent events which results in major rise in pressure and with an increase in the disturbed area which causes to expand. When rise in pressure exceeds a minimum value, a "shock front" is developed and the flow in neighbouring front is referred as "shock wave". The problem of interstellar gas clouds with shock waves has been addressed by various authors. Zeidan et al. [124] discussed the interaction of acceleration and shock waves at stellar surfaces using Lie's method. Jena and Mittal [125] investigated the application of singular surface theory using the method of Lie group transformation. The authors in Gupta and Jena [126] have studied the propagation of strong shocks using the kinematics of one-dimensional shocks and also explored the nature of heating-cooling function on shocks. Bisnovatyi-Kogan and Silich [127] introduced numerical and analytical methods of evolutionary shocks in non-homogeneous interstellar medium. Bedogni and Woodward [128] had provided a detailed description of the interaction of interstellar gas cloud with the shock wave. Heathcode and Brand [129] have discussed the interaction of supernova blast with the interstellar cloud. Ferraioli et al. [130] had studied gravitational collapse of interstellar gas cloud using the propagating theory of wave, and analyzed the role of heating cooling function in the formation of the shock wave. Sharma and Arora[131] have studied the interconnection between acceleration wave and characteristic shock and observed the effect of non-ideal parameters on acceleration wave amplitude. In an interstellar dusty gas cloud, the evolution of weak and strong shocks is analyzed by Chauhan and Arora [132]. Also, the effect of heating-cooling parameters is shown graphically. Singh et al. [133] have studied the effect of non-idealness on evolutionary behavior of shocks using compatibility conditions and truncation procedure. The formation of shocks in a gravitating atmosphere is discussed by Chauhan and Arora [132].

In the present work, the evolution of weak discontinuities has been studied using the method of characteristics for one-dimensional motion of an inviscid, self-gravitating interstellar medium. In continuum mechanics, the weak discontinuity waves are known as acceleration waves. They have continuous solution and discontinuities occur in the solution's derivative along the characteristics. Weak discontinuities occur in numerous mediums, and we observe that their amplitudes follow the subsequent differential equation.

$$\frac{dY}{dt} = -\alpha Y + \delta Y^2, \; 0 \leq t \leq \infty,$$

presents Bernoulli equation, where Y denotes the amplitude of the discontinuity. Generally, α and δ are the functions of time t. The solution of Bernoulli's equation is required for the complete analysis of the flow profile of weak discontinuities. As we are able to obtain the amplitude of the weak discontinuity closely without any approximations, despite of working with a completely nonlinear system, this is the main reason why weak discontinuities are especially useful. The evolution equation for planar and non-planar shocks is derived in interstellar gas clouds. Majorly, our motive is to study how acceleration waves are steepened or flattened after the formation of shock wave and to discuss the impact of cooling heating function and self-gravitating parameter on the nature of the solution. As per our knowledge, the study of the propagation of shock wave in interstellar gas clouds under the impact of van der Waals gas have not been investigated yet by any researcher whereas it has wide application in astronomical problems, star formation, cloud collapse phenomena, formation of stellar systems and in many more problems.(See [[134], [135], [126]])

The description of this chapter is outlined as follows: The governing system of equations and characteristic curves that represent the wave propagation is introduced in part 3.2. In the next part, characteristic variables are introduced and we obtain the solution of acceleration waves to investigate the shock formation process. Part 3.4 contains a detailed analysis of various parameter effects on the formation and distortion of waves. The last part contains the conclusions of this study.

3.2 Wave Propagation

The basic equations governing the one-dimensional flow with inviscid, self-gravitating, and interstellar gas clouds, may be given by (Ferraioli et al. [130], Gupta and Jena [126], Singh et al. [133])

$$\begin{aligned}
&\frac{\partial \rho}{\partial t} + u\frac{\partial \rho}{\partial x} + \rho\frac{\partial u}{\partial x} + \frac{m\rho u}{x} = 0,\\
&\rho\left(\frac{\partial u}{\partial t} + u\frac{\partial u}{\partial x}\right) + \frac{\partial p}{\partial x} = g,\\
&\frac{\partial p}{\partial t} + u\frac{\partial p}{\partial x} + \rho a^2\left(\frac{\partial u}{\partial x} + \frac{mu}{x}\right) = \frac{-(\gamma-1)\rho L(p,\rho)}{(1-b\rho)},\\
&\frac{\partial g}{\partial t} + u\frac{\partial g}{\partial x} = -\frac{mgu}{x}.
\end{aligned} \tag{3.1}$$

Here, m=0,1,2 corresponds to planar, cylindrically symmetric and spherically symmetric flows respectively. The radial distance taken from the origin, time, density, pressure, acceleration due to gravity, van der Waals gas co-volume, ratio of specific heat at constant pressure to specific heat at constant volume, velocity and the net volumetric cooling rate which has been introduced to take into account energy loss and gain mechanisms are denoted by x, t, ρ, p, g, b, γ, u and $L(p,\rho)$ respectively. An equilibrium state for heating/cooling is supposed, with L = 0, for the initial condition, i.e., no net gain or loss of energy. Positive or negative values of $L(p,\rho)$ represents the cooling or heating of the non-ideal interstellar medium. The sound speed 'a' is defined as

$$a = \sqrt{\frac{\gamma p}{(1-\bar{b})\rho}}, \quad here \quad \bar{b} = b\rho.$$

Since we are mainly focused on the dynamical aspects of the problem, our function $L(p, \rho)$ does not take into account sophisticated chemistry, as it is a linear combination of the following processes [Hunter [136]]

$L = A_{ei} + A_g + A_{H_2} - B_{CR} - B_{ph} + A_H + C$ (erg $cm^3\ s^{-1}$), where

$$A_{ei} = \frac{n_H * n_e}{\sqrt{T} * 10^{23}}(64 \times 10^{-2} e^{-92/T} + 17 \times 10^{-1} e^{-554/T} + 64 \times 10^{-1} e^{-413/T} + 22 \times 10^{-1} e^{-961/T}), \quad (ionic\ cooling),$$

$$A_g = \begin{cases} 137 \times 10^{-31} \epsilon n_H \times n_H \times T^{1/2}, & (T > 180^\circ K) \\ 733 \times 10^{-34} \epsilon n_H \times n_H \times T^{1/2} \times (T - T_g), & (T \leq 180^\circ K), \ (inelastic\ collisions) \\ or & \\ 0, & (elastic\ collisions), \end{cases}$$

$$A_{H_2} = 845 \times 10^{-26} n_{H_2} e^{-502/T} \times \{1 + \frac{42}{n_H T^{1/2}(1 + 0.1 n_{H_2}/n_H)}\}^{-1} \quad (H_2\ cooling),$$

$$B_{CR} = 16 \times 10^{-12} F n_H \left(1 + 2\frac{n_{H_2}}{n_H}\right) \ (heating\ of\ cosmic\ ray),$$

$$B_{ph} = 482 \times 10^{-28} n_H n_e T^{0.6548} \ (heating\ of\ photo-ionization),$$

$$A_H = 3 \times 10^{-24} \times T^{-1/2} e^{-227/T} n_H \times n_e \ \ (cooling\ of\ hydrogen\ atom),$$

$$C = -38 \times 10^{-30} \times T^{-1/2} n_H \times n_H e^{-23.6/T} \ (other\ atomic\ cooling\ processes).$$

Here, n_g, n_H and n_e denote the number of interstellar grain, number of hydrogen molecules and electron number density, respectively. F and T_g denotes cosmic ray flux and temperature of the grains , ϵ is the free parameter.

Equation of state for non-ideal gas is

$$p = \frac{\rho RT}{(1 - b\rho)}. \tag{3.2}$$

Here, R and T represent the gas constant and temperature, respectively. We can write equation (3.1) as follows

$$U_t + AU_x + B = 0, \tag{3.3}$$

where U and B are 4×1 ordered column vectors and A is 4×4 ordered matrix, shown below

$$U = \begin{pmatrix} \rho \\ u \\ p \\ g \end{pmatrix}, \quad B = \begin{pmatrix} \frac{m\rho u}{x} \\ -g \\ \frac{m\rho a^2 u}{x} + \frac{(\gamma-1)\rho L}{1-b\rho} \\ \frac{mgu}{x} \end{pmatrix}, \text{and} \quad A = \begin{pmatrix} u & \rho & 0 & 0 \\ 0 & u & 1/\rho & 0 \\ 0 & \rho a^2 & u & 0 \\ 0 & 0 & 0 & u \end{pmatrix},$$

The function $U(x,t)$ satisfying equation (3.3), is continuous everywhere but its derivatives U_t and U_x may suffer finite jump along the characteristic curve $C(t)$ and it is called weak discontinuity. Now, along $C(t)$, we get

$$\frac{\partial}{\partial t}[U] = [U_t] + \frac{dC(t)}{dt}[U_x], \tag{3.4}$$

where $\frac{\partial}{\partial t}$ denotes time derivative.

Since, U is a continuous function, therefore $[U] = 0$.

Taking jump in (3.3) and combining (3.4) with $[U] = 0$ we obtain

$$\left(A - \frac{dC}{dt}I\right)[U_x] = 0. \tag{3.5}$$

From (3.5), we can see that the characteristic speed of propagation $\frac{dC}{dt}$ is an eigenvalue of the matrix A along the characteristic curve $C(t)$. The characteristic curves for (3.3) are as follows:

$$\frac{dx}{dt} = u, \tag{3.6}$$

and

$$\frac{dx}{dt} = u \pm a, \tag{3.7}$$

represents the path of the particle and wave propagation in $\pm\ x$ direction respectively.

3.3 Acceleration waves solution

We introduce ξ and ϕ as two characteristic variables and use them as a frame of reference where ξ and ϕ are particle tag and wave tag respectively with ξ being constant over the particle path $\frac{dx}{dt} = u$ and ϕ being constant across the characteristic $\frac{dx}{dt} = u + a$. So, the particle tag ξ can be marked as $\xi = t^*$ if the characteristic wavefront passes through the particle at time t^*, and the wave tag ϕ can be written as $\phi = t'$ if the outgoing wave is formed at time t'.

Thus, for each pair (ϕ, ξ), we can get a pair (x, t) as $x = x(\phi, \xi)$, $t = t(\phi, \xi)$ such that ϕ and ξ satisfies

$$x_\phi = ut_\phi, \qquad x_\xi = (u+a)t_\xi. \tag{3.8}$$

With the help of (3.8), we can transform U_t and U_x as

$$U_t = \frac{U_\xi x_\phi - U_\phi x_\xi}{J}, \qquad U_x = \frac{U_\phi t_\xi - U_\xi t_\phi}{J}, \tag{3.9}$$

where $J = \dfrac{\partial(x,t)}{\partial(\phi,\xi)} = -Ct_\phi t_\xi$, is the Jacobian of transformation.
Using (3.9) in (3.1) we get

$$a\rho_\phi t_\xi - \rho\left(u_\phi t_\xi - u_\xi t_\phi - \frac{muat_\phi t_\xi}{x}\right) = 0, \tag{3.10}$$

$$a\rho u_\phi t_\xi - p_\phi t_\xi + p_\xi t_\phi = ga\rho t_\phi t_\xi, \tag{3.11}$$

$$ap_\phi t_\xi - \rho a^2(u_\phi t_\xi - u_\xi t_\phi - \frac{muat_\phi t_\xi}{x}) = \frac{-(\gamma-1)\rho L(\rho,p)at_\xi t_\phi}{1-b\rho}, \tag{3.12}$$

$$g_\phi = -\frac{mgut_\phi}{x}. \tag{3.13}$$

Using equations. (3.11) – (3.13) in (3.10), we obtain

$$p_\xi - ga\rho t_\xi + \rho au_\xi + \frac{m\rho a^2 ut_\xi}{x} = \frac{-(\gamma-1)\rho L(\rho,p)t_\xi}{1-b\rho}. \tag{3.14}$$

The boundary conditions at $\phi = 0$ are

$$[\rho] = 0,\ \ [u] = 0,\ \ [p] = 0,\ \ [g] = 0,\ \ [L] = 0,\ \ t = \xi. \tag{3.15}$$

Since, the flow ahead of wave is homogenous and at rest, we observe from (3.15)

$$p_\xi = 0,\ u_\xi = 0,\ \rho_\xi = 0,\ L_\xi = 0,\ g_\xi = 0 \text{ and } t_\xi = 1 \text{ at } \phi = 0. \tag{3.16}$$

At $\phi = 0$, using (3.15) and (3.16) in (3.13), (3.11) and (3.8) we get

$$\rho_\phi = \left(\frac{\rho_0}{a_0}\right) u_\phi, \tag{3.17}$$

$$p_\phi = \rho_0 a_0 u_\phi, \tag{3.18}$$

$$x_\phi = 0, \quad x_\xi = a_0. \tag{3.19}$$

The flow variables estimated ahead of the wave are indicated by the subscript '0'. Using (3.16) in (3.9), we get

$$\left[\frac{\partial u}{\partial x}\right] = X = -\frac{u_\phi}{a_0 t_\phi}, \quad \text{at } \phi = 0, \tag{3.20}$$

where X is amplitude of weak discontinuity waves at $\phi = 0$.

Next we will determine the dependence of u_ϕ and t_ϕ on time. Differentiating (3.8), (3.14) and (3.18) with respect to ϕ and ξ, at $\phi = 0$, we get

$$\frac{t_{\phi\xi}}{t_\phi} = \frac{\gamma + 1}{2(1 - \bar{b})} X, \tag{3.21}$$

$$\frac{u_{\phi\xi}}{t_\phi} = \frac{a_0}{2} \frac{\gamma - 1}{a_0^2 (1 - \bar{b})^2} (\frac{(1 - \gamma)}{2} L_0 + (L_{\rho_0} + a_0^2 L_{p_0}) \rho_0 (1 - \bar{b})) \frac{g_0(\gamma - 1)}{2a_0(1 - \bar{b})} + \frac{m a_0}{\xi}, \tag{3.22}$$

where the quantities L_{ρ_0} and L_{p_0} represents partial differentiation of L with respect to ρ and p respectively. The subscript 'zero' denotes physical quantities ahead of the shock.

Differentiating (3.20) with respect to ξ and using (3.21) and (3.22), we get

$$\frac{dX}{d\xi} + \left(\frac{\gamma-1}{2(1-\bar{b})a_0^2}\left((\frac{1-\gamma}{2})L_0 + (L_{\rho_0} + a_0^2 L_{p_0})\rho_0(1-\bar{b})\right) + \frac{g_0(\gamma+1)}{4a_0(1-\bar{b})} + \frac{ma_0}{2\xi}\right)X$$
$$+ \left(\frac{\gamma+1}{2(1-\bar{b})}\right)X^2 = 0, \text{ at } \phi = 0. \tag{3.23}$$

Now, we introduce following non-dimensional quantities given as

$$\chi = \frac{X}{X^*}, \quad \psi = \frac{\xi - \xi^*}{2\xi^*} \text{ and } \delta = X^*\xi^*. \tag{3.24}$$

Here, δ, χ, and ψ are the initial disturbance, wave amplitude, and time, respectively. The superscript '*' has been used to denote the parameter's value at $t = t^*$.

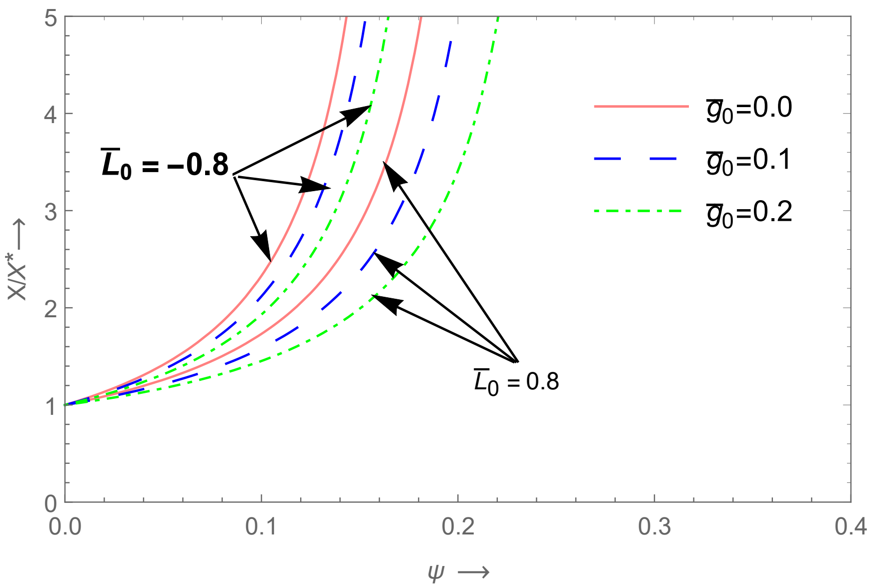

FIGURE 3.1: Effect of self gravitating parameter $\overline{g_0}$ for $\delta < 0$ with $\gamma = 1.67, \delta = -1.5, m = 0$ (*planar case*)$, \bar{b} = 0.3$.

Considering equation (3.24), equation (3.23) can be reduced to the following dimensionless form

$$\frac{d\chi}{d\psi} + \left(\frac{\overline{L_0} + \overline{g_0}}{(1-\bar{b})} + \frac{m}{2\psi+1}\right)\chi + \frac{\delta(\gamma+1)}{(1-\bar{b})}\chi^2 = 0, \;\text{ at } \phi = 0. \tag{3.25}$$

where

$$\overline{L_0} = \frac{(\gamma-1)}{a_0^2}\left(\frac{(1-\gamma)L_0}{1-\bar{b}}\right) + (L_{\rho_0} + a_0^2 L_{p_0}))\xi^*, \tag{3.26}$$

$$\overline{g_0} = \frac{(\gamma+1)g_0\xi^*}{2a_0}, \tag{3.27}$$

$\overline{L_0}$ and $\overline{g_0}$ denotes net volumetric cooling rate and self gravitating parameter respectively.

The solution of equation (3.25) is

$$\chi = \left\{(2\psi+1)^{\frac{m}{2}} e^{\left(\frac{R_0}{(1-\bar{b})}\right)\psi}\left(1 + \left(\frac{(\gamma+1)\delta}{(1-\bar{b})}J(\psi)\right)\right)\right\}^{-1}, \tag{3.28}$$

where $J(\psi) = \int_0^\psi \frac{-e^{\left(\frac{\overline{L_0}+\overline{g_0}}{(1-\bar{b})}\right)s}}{(2s+1)^{\frac{m}{2}}} ds.$

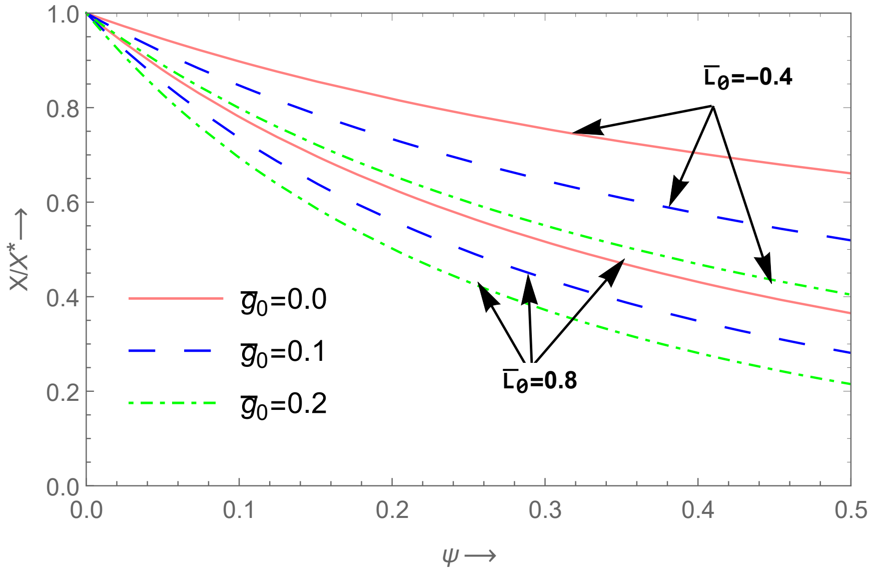

FIGURE 3.2: Effect of self gravitating parameter $\overline{g_0}$ for $\delta > 0$ with $\gamma = 1.67, \delta = 0.5, m = 0$ (*planar case*)$, \bar{b} = 0.3$.

From equations (3.20) and (3.28), it is clear that, for the formation of shock we must have $t_\phi = 0$, i.e.

$$1 + \left(\frac{(\gamma+1)\delta}{(1-\bar{b})} J(\psi) \right) = 0. \tag{3.29}$$

The function $J(\psi)$ plays a significant role in the breakdown of characteristic solution. From (3.29) it is clear that the compressive waves $(\delta < 0)$ end into the shock waves.

3.4 Growth and decay of acceleration wave

We now investigate the behavior of the earlier obtained solution and examine the effect of parameters on the formation and deformation of the shocks by considering three cases for three different values of m. In computations, numerical values used are $\gamma = 1.67$ [Ogino et al. [137]], $\delta = -1.5$ *or* 0.5, $\bar{b} = 0.3$ [Chaturvedi et al. [94], Srivastava et al. [97]]. Using the computational package MATHEMATICA, all the computations are performed.

Case I. Planar flow $(m = 0)$**:**

Substituting $m = 0$ in (3.28), we obtain the solution of (3.25) as

$$X = \frac{X^*}{e^{\left(\frac{\overline{L_0}+\overline{g_0}}{(1-\overline{b})}\right)\psi}\left(1+\left(\frac{(\gamma+1)\delta}{(1-\overline{b})}J(\psi)\right)\right)}, \tag{3.30}$$

where, $J(\psi) = \int_0^{\psi} -e^{\left(\frac{\overline{L_0}+\overline{g_0}}{(1-\overline{b})}\right)s} ds.$

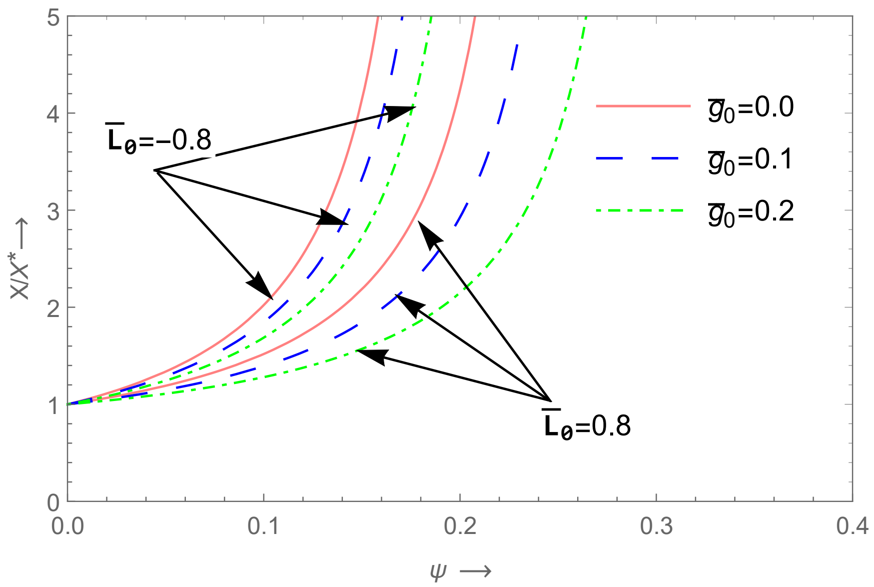

FIGURE 3.3: Effect of self gravitating parameter $\overline{g_0}$ for $\delta < 0$ with $\gamma = 1.67, \delta = -1.5, m = 1$ (*cylindrical case*)$, \overline{b} = 0.3$.

Fig.3.1 represents the solution curve for compressive wave, exibiting shock formation and increase in the value of self gravitating parameter results in delay in formation of shocks. It is clear from graph that shock forms early in case of heating function effect in comparison to cooling function effect but it decelerates with rise in $\overline{g_0}$. Fig.3.2 shows expansive wave solution curves which clearly depicts that it does not exhibit the shock formation but decays out. With rise in $\overline{g_0}$, decay rate of propagation increases and the effect of cooling function causes to decay faster in comparison to heating function effect.

Case II. Cylindrically symmetric flow $(m = 1)$**:**

Placing $m = 1$ in (3.28), we obtain solution of (3.25) as

$$X = \frac{X^*}{(2\psi + 1)^{1/2} e^{\left(\frac{\overline{L_0}+\overline{g_0}}{(1-\bar{b})}\right)\psi} \left(1 + \left(\frac{(\gamma+1)\delta}{(1-\bar{b})} J(\psi)\right)\right)}, \tag{3.31}$$

where, $J(\psi) = \int_0^{\psi} \frac{-e^{\left(\frac{\overline{L_0}+\overline{g_0}}{(1-\bar{b})}\right)s}}{(2\psi+1)^{1/2}} ds.$

In this case, the nature of solution curves is more or less same as that of those for planar flow. Fig.3.3 displays shock formation and with rise in $\overline{g_0}$ there is delay in formation of shocks. The growth rate of the compressive wave is lower in case of cooling function effect, than that of heating gas cloud effect ($\overline{L_0} < 0$). Fig3.4 depicts that the decay rate of propagation of the expansive wave enhances. It can be seen from the graph that the decay rate of the expansive wave is higher in the case of a cooling gas cloud, i.e, $\overline{L_0} > 0$ than that of heating gas cloud effects ($\overline{L_0} < 0$).

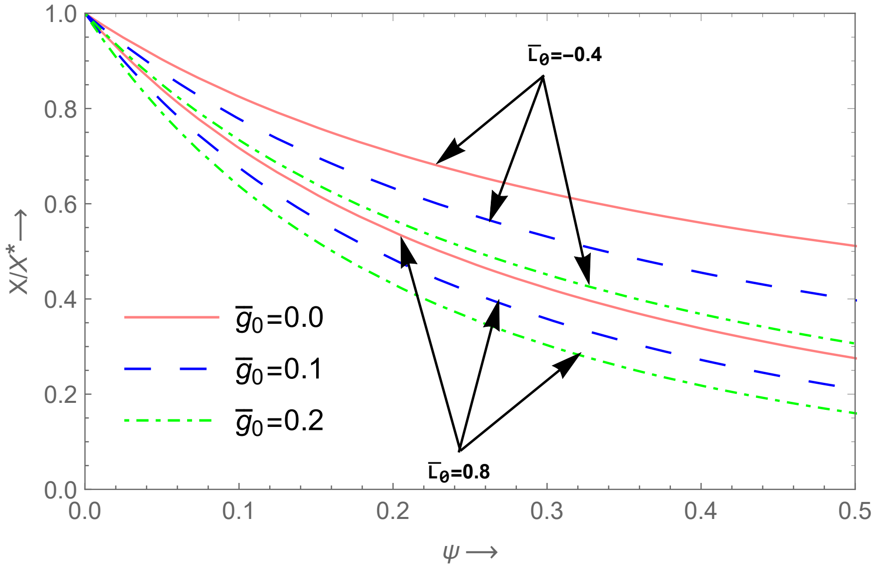

FIGURE 3.4: Effect of self gravitating field $\overline{g_0}$ for $\delta > 0$ with $\gamma = 1.67, \delta = 0.5, m = 1$ (*cylindrical case*), $\bar{b} = 0.2$.

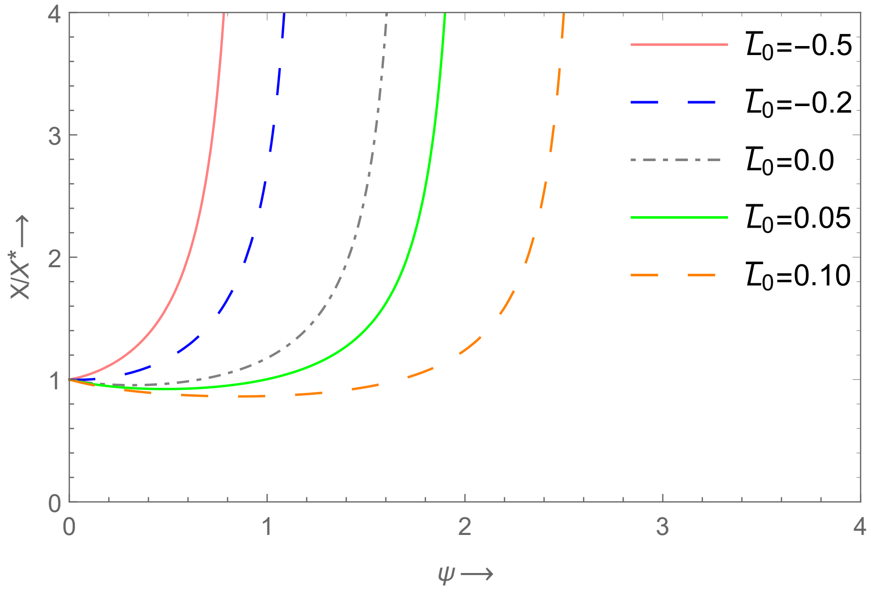

FIGURE 3.5: Effect of net volumetric cooling rate $\overline{L_0}$ for $\delta < 0$ with $\delta = -0.5, \gamma = 1.67, m = 1$ (*cylindrical case*), $\bar{b} = 0.3$.

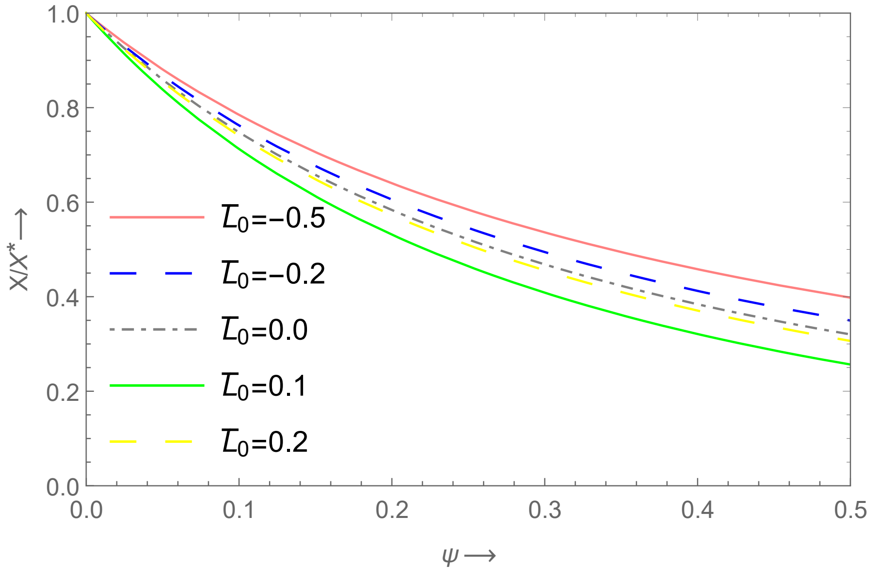

FIGURE 3.6: Effect of net volumetric cooling rate $\overline{L_0}$ for $\delta > 0$ with $\delta = 0.5, \gamma = 1.67, m = 1$ (*cylindrical case*), $\bar{b} = 0.3$.

Fig.3.5 depicts compressive wave's growth behavior and observed that with rise in $\overline{L_0}$, there is delay in formation of shock. The growth rate is very slow in the case of cooling of gas cloud $\overline{L_0} > 0$ as compared to heating of gas cloud $\overline{L_0} < 0$. Fig.3.6 shows the decay rate of expansive wave which clearly depicts that it does not exhibit the shock formation and with rise in $\overline{L_0}$, the decay rate of the expansive wave rises. The decay rate is more in cooling gas cloud as compared to heating gas cloud.

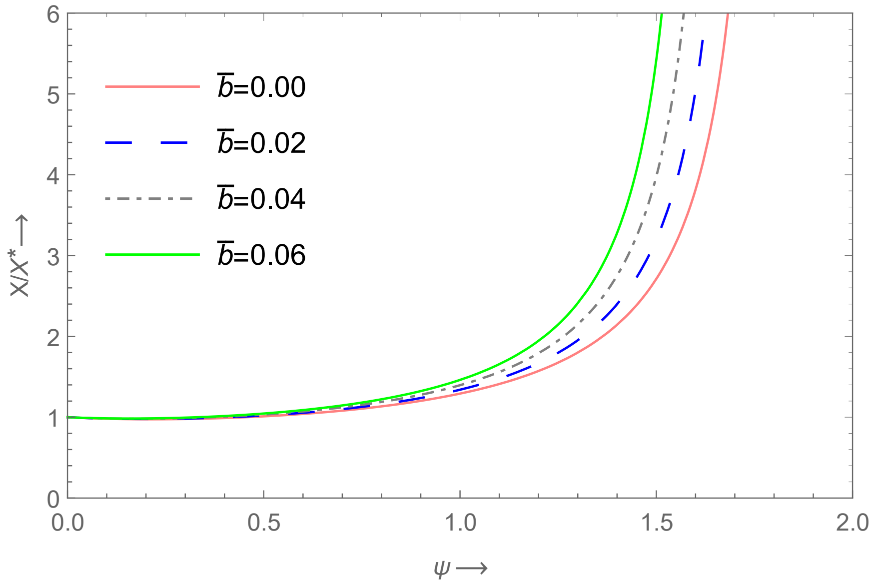

FIGURE 3.7: Effect of non-ideal parameter $\bar{b}$ for $\delta < 0$ with $\overline{L_0}$=0.4, $\overline{g_0}$=0.2, m=1 (cylindrical case), δ=-0.5 .

.

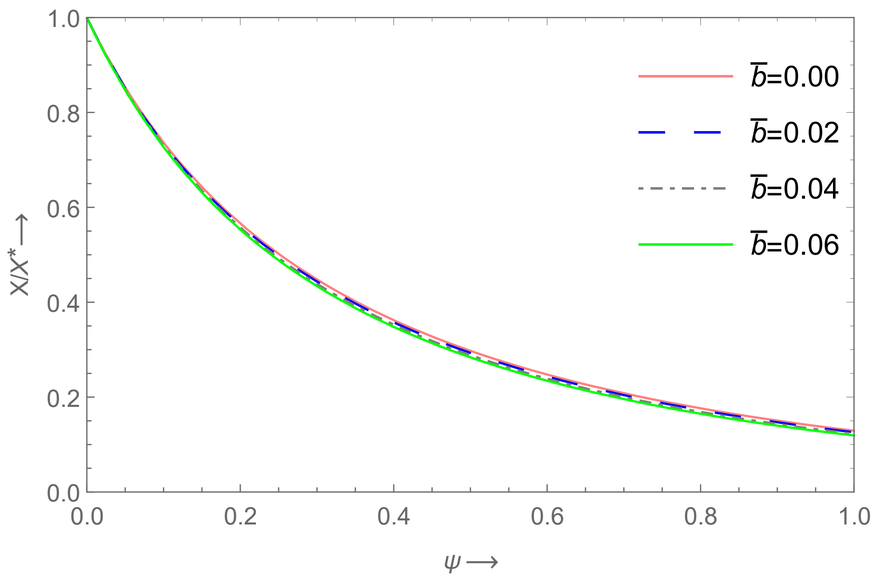

FIGURE 3.8: Effect of non-ideal parameter $\bar{b}$ for $\delta > 0$ $\overline{L_0}$=0.2, $\overline{g_0}$=0.8, m=1 (cylindrical case), δ=0.5 .

Fig.3.7 depicts the impact of $\bar{b}$ and rise in its values results in an early formation of shock. Fig.3.8 displays that the decay rate of the expansive wave is faster with rise in the value of $\overline{b}$ but the increase is significantly low.

Case III. Spherically symmetric flow $(m = 2)$**:**

Placing $m = 2$ in (3.28), we obtain solution of (3.25) as

$$X = \frac{X^*}{(2\psi + 1)e^{\left(\frac{\overline{L_0}+\overline{g_0}}{(1-\overline{b})}\right)\psi}\left(1 + \left(\frac{(\gamma+1)\delta}{(1-\overline{b})}J(\psi)\right)\right)}, \tag{3.32}$$

where, $J(\psi) = \int_0^\psi \frac{-e^{\left(\frac{\overline{L_0}+\overline{g_0}}{(1-\overline{b})}\right)s}}{(2\psi+1)} ds.$

The nature of the solution curves in this case is comparable to those for planar and cylindrically symmetric flow cases which is evident from Fig.3.9 and 3.10.

The comparative study for all instances is shown in Fig.3.11 and 3.12 which indicates both compressive and expansive waves for net volumetric cooling rate. From Fig.3.11 it is clear that in planar case shock formation is early in comparison to cylindrically and spherically symmetric case. Clearly compressive wave terminates into shock waves and expansion waves decays out.

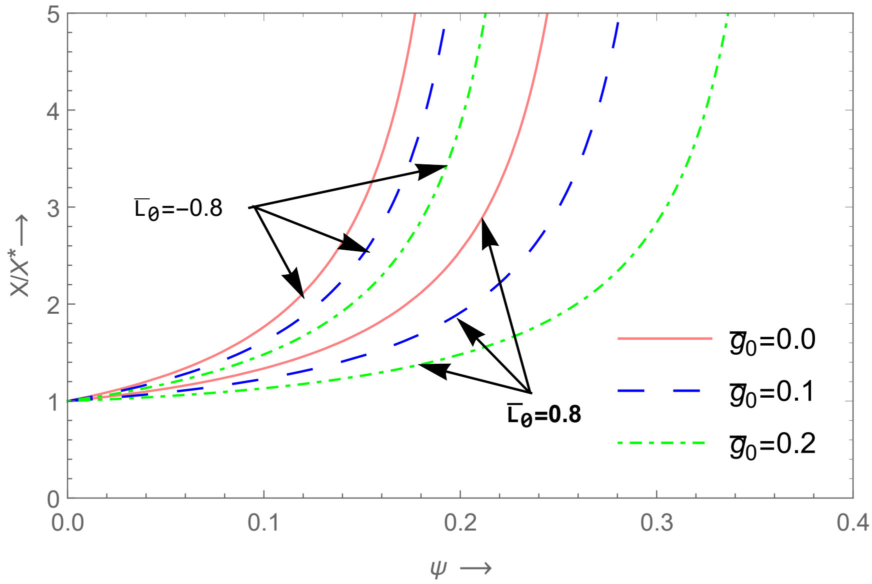

FIGURE 3.9: Effect of self gravitating parameter $\overline{g_0}$ for $\delta < 0$ with $\gamma = 1.67, \delta = -1.5, m = 2$ (*spherical case*), $\overline{b} = 0.3$.

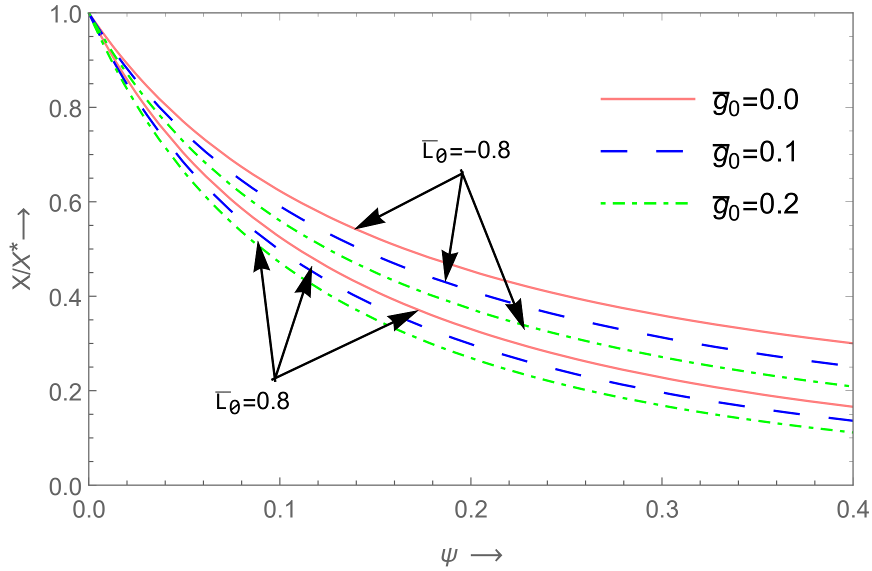

FIGURE 3.10: Effect of self gravitating parameter $\overline{g_0}$ for $\delta > 0$ with $\gamma = 1.67, \delta = 0.5, m = 2$ (*spherical case*), $\overline{b} = 0.3$.

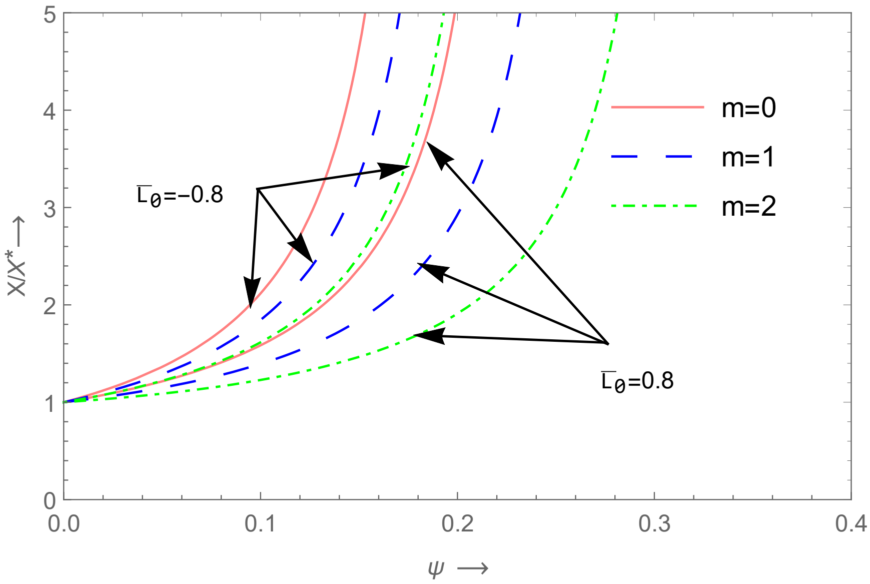

FIGURE 3.11: Comparative study of the geometry of non-ideal interstellar gas cloud for $\gamma = 1.67, \delta = -1.5, \bar{b} = 0.3, \overline{g_0} = 0.5$.

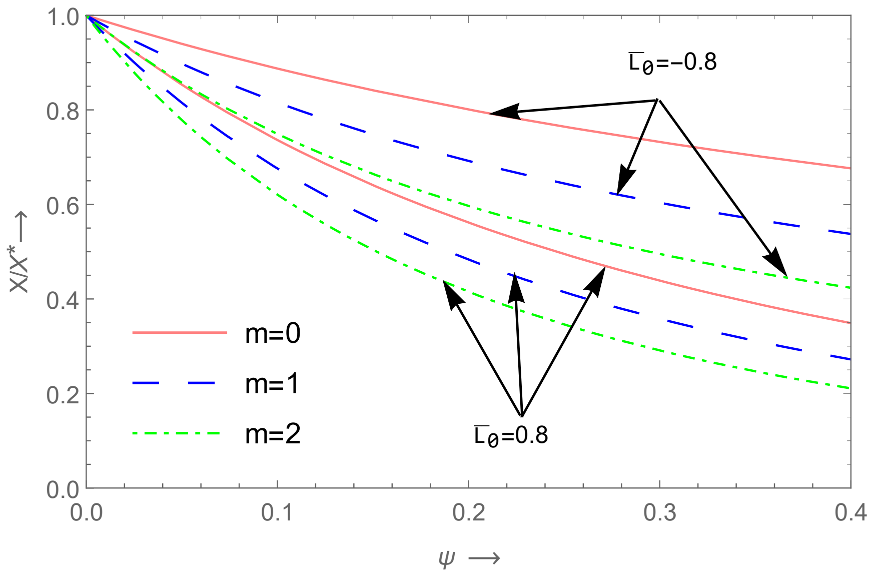

FIGURE 3.12: Comparative study of the geometry of non-ideal interstellar gas cloud for $\gamma = 1.67, \delta = 0.5, \bar{b} = 0.3, \overline{g_0} = 0.5$.

3.5 Conclusion

This chapter describes an analytical method for determining the solution of problem of shock wave propagation for planar, cylindrical, spherical flow of hyperbolic system governing a one-dimensional inviscid flow in self-gravitating, non-ideal interstellar gas cloud. The propagation of weak discontinuity waves along the characteristic are studied using the characteristic method. We found that expansive wave will exponentially decay in amplitude and will be damped out ultimately. The non-adiabatic and thermal behaviour of the interstellar gas is the most important single factor influencing star formation. In the interior of clouds, that are effectively shielded from the galactic ultraviolet radiation field by interstellar grains, molecular hydrogen is an important cooling agent. Self gravitation plays an important role in the fields of astronomy, seismology, geology and oceanography. The influence of self-gravitating parameter on shock formation is examined and we analyzed that it causes to accelerate the decay process of expansive waves and slow down the growth rate of compressive waves in the non-ideal interstellar gas cloud. Also, decaying of expansive wave is higher in the case of cooling gas cloud than that of heating gas cloud effect, and growth of compressive wave is lower in case of cooling gas cloud than that of heating gas cloud effect. For cylindrically symmetric case, it is examined how the shock wave solution is influenced by the presence of van der Waals excluded volume and net volumetric cooling rate in the interstellar gas cloud. For more clarifications, a comparative study of planar and non-planar case is done and it is observed that there is delay in the formation of shocks in spherically symmetric case shown in Fig. 3.11.

****